Identity, regulation, and activity of inducible diterpenoid phytoalexins in maize

Eric A. Schmelz[a,1], Fatma Kaplan[a], Alisa Huffaker[a], Nicole J. Dafoe[a], Martha M. Vaughan[a], Xinzhi Ni[b], James R. Rocca[c], Hans T. Alborn[a], and Peter E. Teal[a]

[a]Chemistry Research Unit, Center of Medical, Agricultural, and Veterinary Entomology, US Department of Agriculture, Agricultural Research Service, Gainesville, FL 32608; [b]Crop Genetics and Breeding Research Unit, US Department of Agriculture, Agricultural Research Service, Tifton, GA 31793; and [c]Advanced Magnetic Resonance and Imaging, McKnight Brain Institute, University of Florida, Gainesville, FL 32610

Phytoalexins constitute a broad category of pathogen- and insect-inducible biochemicals that locally protect plant tissues. Because of their agronomic significance, maize and rice have been extensively investigated for their terpenoid-based defenses, which include insect-inducible monoterpene and sesquiterpene volatiles. Rice also produces a complex array of pathogen-inducible diterpenoid phytoalexins. Despite the demonstration of fungal-induced *ent*-kaur-15-ene production in maize over 30 y ago, the identity of functionally analogous maize diterpenoid phytoalexins has remained elusive. In response to stem attack by the European corn borer (*Ostrinia nubilalis*) and fungi, we observed the induced accumulation of six *ent*-kaurane–related diterpenoids, collectively termed kauralexins. Isolation and identification of the predominant *Rhizopus microsporus*-induced metabolites revealed *ent*-kaur-19-al-17-oic acid and the unique analog *ent*-kaur-15-en-19-al-17-oic acid, assigned as kauralexins A3 and B3, respectively. Encoding an *ent*-copalyl diphosphate synthase, fungal-induced *An2* transcript accumulation precedes highly localized kauralexin production, which can eventually exceed 100 $\mu g \cdot g^{-1}$ fresh weight. Pharmacological applications of jasmonic acid and ethylene also synergize the induced accumulation of kauralexins. Occurring at elevated levels in the scutella of all inbred lines examined, kauralexins appear ubiquitous in maize. At concentrations as low as 10 $\mu g \cdot mL^{-1}$, kauralexin B3 significantly inhibited the growth of the opportunistic necrotroph *R. microsporus* and the causal agent of anthracnose stalk rot, *Colletotrichum graminicola*. Kauralexins also exhibited significant *O. nubilalis* antifeedant activity. Our work establishes the presence of diterpenoid defenses in maize and enables a more detailed analysis of their biosynthetic pathways, regulation, and crop defense function.

Fusarium graminearum | 10-oxo-11-phytoenoic acid | benzoxazinoid hydroxamic acid

Phytoalexins are defined as low-molecular-weight, inducible, secondary metabolites with activity against multiple biotic attackers. Terpenoids, including sesquiterpenes and diterpenes, constitute some of the commonly encountered chemical classes of phytoalexins (1). In cotton (*Gossypium hirsutum*), pathogens and insect herbivores trigger synthesis of the sesquiterpene δ-cadinene and numerous subsequent oxidation products, which, collectively, afford protection against these attackers (2, 3). Similarly, in rice (*Oryza sativa*), pathogen infection induces the levels of transcripts encoding key biosynthetic enzymes, namely, an *ent*-copalyl diphosphate synthase (*ent*-CPS; OsCPS2) and a *syn*-CPS (OsCPS4), which lead to diterpenoid phytoalexin production (4). These inducible diterpenoids have established roles in protecting against the ascomycete fungus *Magnaporthe grisea*, the causal agent of rice blast disease, which is responsible for 10–30% of losses in production (5).

Maize is the largest crop on earth, with over 810 million tons of seed harvested in 2009 (6). To improve crop protection, maize has been widely studied for its production of terpenoid volatiles and benzoxazinoid hydroxamic acids as two major classes of bio-

chemical resistance (7). As indirect defenses, inducible terpenoid volatiles have been demonstrated to attract parasitoids and entomopathogenic nematodes to above- and below-ground insect pests, respectively (8, 9). As a direct defense, the largely constitutive hydroxamic acids in maize are responsible for *Ostrinia nubilalis* leaf-feeding resistance in young plants (7). Upon moving to stems, *O. nubilalis* tunneling creates a contaminated and humid environment for microbial colonization. Not surprisingly, *O. nubilalis* damage is highly associated with stalk rot pathogens, including *Colletotrichum graminicola* and *Fusarium* spp. (10, 11). Keller et al. (11) summarized this relationship, stating that "Consequently, any yield reduction studies, breeding programs, or other control strategies focusing on a single fungus or insect would be incomplete without detailed consideration of the concomitant role of other pests." The elucidation of maize defense mechanisms remains a topic of significant interest, given that the combined pressures of *O. nubilalis* and stalk rot pathogens have resulted in $1 billion annual losses in US production alone (12, 13).

To combat pathogens, rice produces numerous classes of inducible diterpenoids, including the oryzalexins, momilactones, and phytocassanes, each of which is produced by a unique class of kaurene synthases (4). A rice cultivar with constitutive bacterial leaf blight resistance, Norin-27, was also used to isolate a series of oryzalide-related defense compounds that occur constitutively in healthy leaves (14). These diterpenoids are likely derived from the kaurene synthase OsKSL6 via an *ent*-kaur-15-ene intermediate (4). Although diterpenoid phytoalexins have not been previously demonstrated in maize, *ent*-kaur-15-ene is synthesized following infection with fungi from the genera *Rhizopus* and *Fusarium*; however, this simple maize hydrocarbon is not antimicrobial (15). Further tangential evidence for maize diterpenoid phytoalexins comes from the discovery that *Fusarium graminearum* infection strongly induces transcript accumulation of *An2*, which encodes a functional *ent*-CPS that is unlikely to be involved in the biosynthesis of gibberellins (GAs) (16, 17).

Elicitors present in the oral secretions of insect herbivores commonly induce terpenoids in the leaves of plants (18). To explore related defensives in maize stems, we examined *O. nubilalis*-induced metabolites. Initially, two unknown diterpene acids were detected that were also induced following fungal spore inoculation. A large-scale isolation and NMR-based identification project revealed series of *ent*-kaurane–related diterpenoids, with *ent*-kaur-19-al-17-oic acid and the unique analog *ent*-kaur-15-en-19-al-17-oic acid as the major induced defenses. Localized accumulation of

PLANT BIOLOGY

these inducible diterpenoids, termed kauralexins, is preceded by transcript accumulation of *An2*. A combination of the phytohormones jasmonic acid (JA) and ethylene (E) has a synergistic role in this regulation. Importantly, physiologically relevant concentrations of kauralexins inhibit the growth of pathogens and display insect antifeedant activity. Similar to rice, maize harbors highly inducible diterpenoid phytoalexins that are likely to have essential roles in crop protection.

Results and Discussion

Identity of *ent*-Kaurane–Related Phytoalexins in Maize. To understand induced defenses in maize stems better, we performed small-molecule metabolic profiling on feeding tunnels created by *O. nubilalis* larvae (19). Initially, two chromatographic peaks consistent with diterpene acid methyl esters were detected. *Rhizopus microsporus* spore inoculation also strongly induced the concentrations of these and four additional analytes. To identify these compounds, a large-scale purification of fungal infected tissue was performed and resulted in purification of three of the six related compounds enabling structural elucidation via NMR ([SI Text](#) and Tables S1–S3). This information, coupled with the chemical ionization (CI) and electron ionization (EI) spectra of the corresponding methyl ester derivatives, was consistent with closely related *ent*-kaurane diterpenoids, namely, *ent*-kauran-17-oic acid, *ent*-kauran-17,19-dioic acid, and *ent*-kaur-19-al-17-oic acid, termed kauralexins A1 through A3, respectively (Fig. 1 *A–D*). Kauralexin A2 was identified based on the known natural product isolated from the roots of *Annona squamosa* trees (20) (Fig. 1*C* and [Fig. S1](#)).
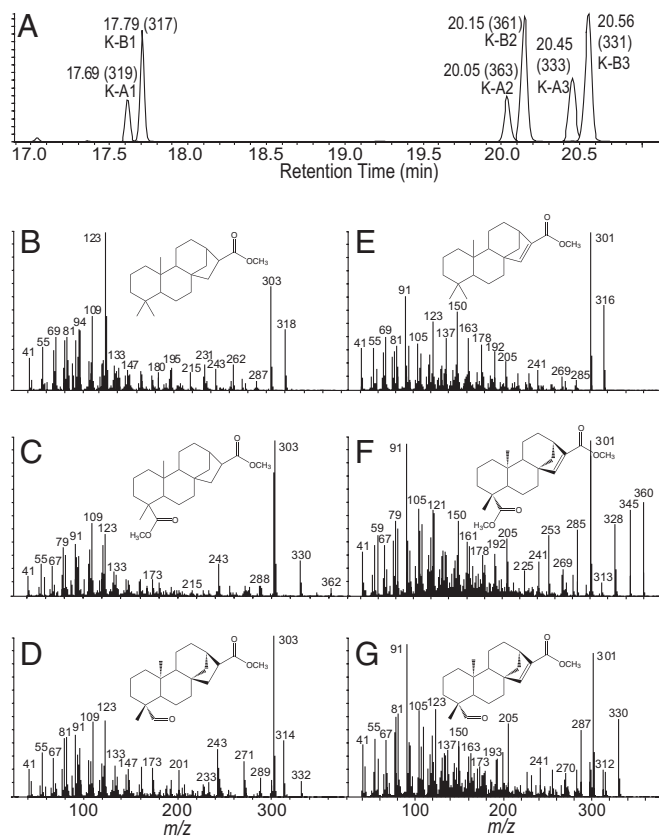

Fig. 1. Identity and GC/MS spectra of kauralexin A1–A3 and B1–B3 methyl esters. (*A*) GC retention times and predominant positive-CI MS [M + H]+ ions of kauralexins A1–A3 and B1–B3 (e.g., K-A1, K-B1) methyl esters. Structures and EI spectra of kauralexins A1 (*B*), A2 (*C*), A3 (*D*), B1 (*E*), B2 (*F*), and B3 (*G*), respectively, are shown as methyl ester derivatives. In each panel, the *y* axis denotes relative abundance of ions.

NMR, CI, and EI spectra were also consistent with a second series of diterpenoids, namely, *ent*-kaur-15-en-17-oic acid, *ent*-kaur-15-en-17,19-dioic acid, and *ent*-kaur-15-en-19-al-17-oic acid, termed kauralexins B1 through B3, respectively (Fig. 1 *A* and *E–G*). Based on coregulation and previously published spectra, we provisionally assigned the saturated and monounsaturated diterpene acids as kauralexins A1 and B1, respectively (21, 22) (Fig. 1 *B* and *E*). Kauralexin B1 is a logical precursor for kauralexin B2/B3 and is likely derived from pathogen-induced *ent*-kaur-15-ene (15). With the exception of kauralexin B3, these diterpenoids have been previously described in dicotyledonous plants; however, kauranes have not been previously established to function as rapidly inducible phytoalexins (20–24). These compounds are readily quantified by GC similar to the routine analysis of fatty acid methyl esters (25). This raises the question of why the identity of maize diterpenoid phytoalexins has escaped attention for so long. A number of factors are involved. First, many of these structures are not commonly known or have only been encountered once in a single plant species (22). Second, kauralexin accumulation is highly localized; thus, harvesting large tissue samples greatly dilutes the abundance of kauralexins and reduces detectability. Third, kauralexins are easily degraded, especially by the high heat and pH extremes commonly used in processing lipid samples (25). During isolation, kauralexin B2 fractions were highly prone to sample loss and could only be purified as methyl ester derivatives.

Insect and Fungal Attack Trigger Kauralexin Accumulation. To address the timing of induced kauralexin accumulation, short- and long-term effects of insect herbivory and fungal infection were examined. Within 48 h of *O. nubilalis* stem herbivory, tissue concentrations of kauralexins A1, B1, B2, and B3 were significantly higher than mechanical damage alone (Fig. 2 *A* and *D–F*). Both *O. nubilalis* herbivory and damage induced low levels of kauralexins A2 and A3 above those of the unwounded controls (Fig. 2 *B* and *C*). After 8 d of *O. nubilalis* herbivory, kauralexin levels averaged 10-fold higher than those found at 48 h (Fig. 2 *A–F* and [Fig. S2*A*](#)). Infection with *C. graminicola* resulted in significant kauralexin accumulation above mechanical damage alone, yet these levels were low compared with those induced by infection with *R. microsporus* (Fig. 2 *G–L*). *R. microsporus* inoculation strongly induced the levels of all six kauralexins above damage alone, *C. graminicola* infection, and pectinase elicitation (Fig. 2 *G–L*). At ~10 μg·g^{-1} fresh weight (FW), kauralexins A3 and B3 were the major diterpenoids accumulated at 24 h (Fig. 2 *I* and *L*). To examine effects at 48 h, plants were also inoculated with the stalk rot, *F. graminearum*. This treatment induced kauralexin levels to 100 μg·g^{-1} FW, a 2,400-fold induction above untreated controls ([Fig. S2*B*](#)). Consistent with many phytoalexins, kauralexins require multiple days to reach maximal accumulation (1).

Phytohormone-Induced Kauralexin Accumulation. Plant defense responses to biotic attack are often mediated by the synergistic phytohormone actions of E and oxylipin signals, such as JA (18, 26, 27). To examine the potential role of induced oxylipins as regulators of kauralexin production, damaged stems were inoculated with *R. microsporus*. This treatment resulted in JA levels significantly greater than damage alone at 4 h, which preceded detectable kauralexin accumulation (Fig. 2 *G–L* and Fig. 3*A*). At later time points, concentrations of additional allene oxide synthase-derived oxylipins, such as the biologically active JA precursor, 12-oxo-phytodienoic acid (OPDA), and its linoleic acid-derived isomer, 10-oxo-11-phytoenoic acid (OPEA), were induced following damage and fungal inoculation, respectively (28, 29) (Fig. 3 *B* and *C*). To examine potential signaling interactions, plants were treated with JA, OPDA, and OPEA in the absence and presence of ethephon (EP; 2-chloroethyl-phosphonic acid), which generates the local production of E (30). The combination of JA and EP significantly
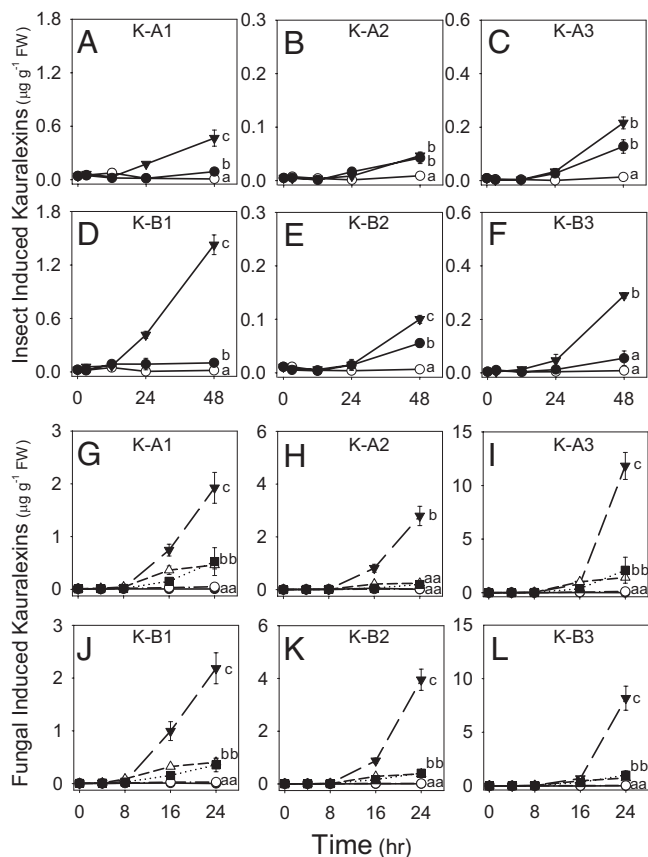
Fig. 2. Insect and fungal attack rapidly induces kauralexin concentrations. Average ($n = 3$, ±SEM) induced kauralexin A1 (*A*), A2 (*B*), A3 (*C*), B1 (*D*), B2 (*E*), and B3 (*F*) concentrations in maize stems experiencing no treatment (○), mechanical damage (●), and *O. nubilalis* herbivory (▼). Average ($n = 4$, ±SEM) induced kauralexin A1 (*G*), A2 (*H*), A3 (*I*), B1 (*J*), B2 (*K*), and B3 (*L*) concentrations in control maize stems (○) or those treated with a combination of damage plus H₂O (●), pectinase elicitor (■), *C. graminicola* spores (△), or *R. microsporus* spores (▼). Because of the similarity between control/damage + H₂O and pectinase/*C. graminicola* treatments, plot symbols are partly obscured. Within plots, different letters (a–c) represent significant differences at final time points ($P < 0.01$ for all ANOVAs; $P < 0.05$ for Tukey test corrections for multiple comparisons).

induced kauralexin concentrations above all other treatments (Fig. 3*D*). To ensure this result was not an artifact, we tested the interaction of JA with the endogenous E precursor, 1-aminocyclopropane-1-carboxylic-acid (ACC), and additional non–E-generating controls. Results confirmed a significant JA-E synergy (Fig. S3 *A* and *B*). These patterns are similar to those found in spruce trees (*Picea* spp.), where insect damage and applications of methyl jasmonate induce traumatic resin duct formation in the developing secondary xylem and promote transcript accumulation of diterpene synthases and diterpene resin acid accumulation (31). This process was inhibited by 1-methylcyclopropene, which blocks E perception, thus implicating the involvement of both JA and E signals (32).

Induced *An2* Transcript Levels Precede Kauralexin Accumulation. In rice, the production of *ent*-copalyl diphosphate as an essential precursor of GAs and phytocassane diterpenoids is controlled by two distinctly regulated enzymes, namely, OsCPS1ₑₙₜ and OsCPS2ₑₙₜ, respectively (33). Maize also contains two different *ent*-CPSs, with an established role for AN1 in GA biosynthesis and a putative role for AN2 in phytoalexin biosynthesis (16, 17). Importantly, *An2* transcript accumulation, but not that of *An1*, is
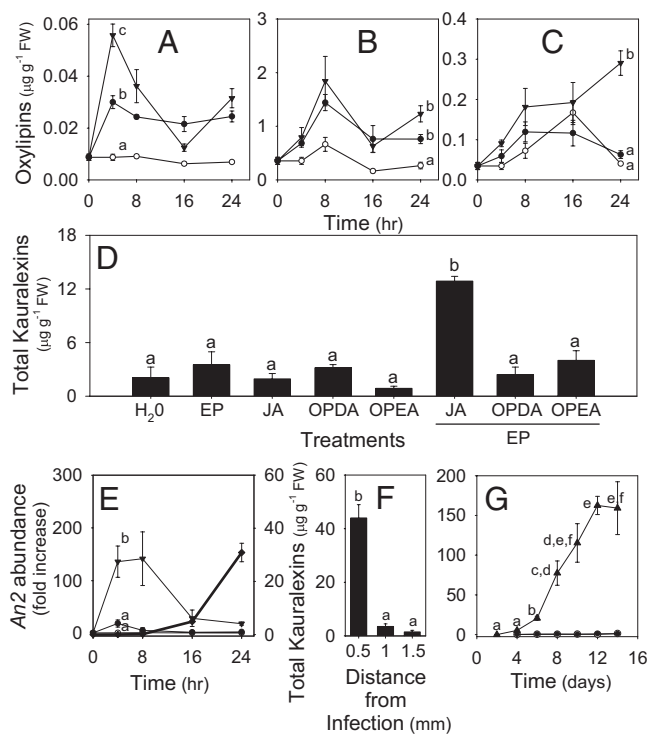

Fig. 3. Insights into hormonal, transcriptional, spatial, and developmental regulation of kauralexins. Average ($n = 4$, ±SEM) trans-JA (*A*), OPDA (*B*), and OPEA (*C*) concentrations in control stems (○) or those treated with a combination of damage plus either H₂O (●) or *R. microsporus* spores (▼). (*D*) Average ($n = 4$, ±SEM) total kauralexins in stems 24 h after treatment with damage plus H₂O, EP, JA, OPDA, OPEA, or a combination of JA + EP, OPDA + EP, and OPEA + EP. (*E*) Average ($n = 3$, ±SEM) qRT-PCR transcript levels of *An2* in control stems (○) or those treated with a combination of damage plus either H₂O (●) or *R. microsporus* spores (▼) and subsequent kauralexin (◆) accumulation. (*F*) Average ($n = 4$, ±SEM) total kauralexins in successively removed layers of *R. microsporus*-inoculated stems. (*G*) Average ($n = 4$, ±SEM) total kauralexin accumulation in the roots (○), shoots (●), and scutella (▲) of healthy untreated seedlings. Within plots, different letters (a–f) represent significant differences at indicated time points ($P < 0.01$ for all ANOVAs; $P < 0.05$ for Tukey test corrections for multiple comparisons).

highly induced by the ear rot pathogen *F. graminearum* and smut fungus *Ustilago maydis* (17, 34). To confirm the presence and functionality of *An2* in var. Golden Queen, the gene was cloned, sequenced, expressed in *Escherichia coli*, and assayed for *ent*-CPS activity. Compared with the maize inbred CO387, Golden Queen *An2* is highly conserved, harbors six amino acid differences in the predicted translation, and maintains *ent*-CPS activity in bacterial expression assays (Fig. S4 *A–C*). To examine the relationship between *An2* and kauralexins, transcript levels following *R. microsporus* inoculation were analyzed by quantitative RT-PCR (qRT-PCR). A 135-fold increase in *An2* levels preceded significant kauralexin accumulation by ~20 h (Fig. 3*E*). A nearly identical temporal relationship has been shown with OSCPS2ₑₙₜ and diterpenoid phytoalexin accumulation in rice (33). Although definitive proof is lacking, these results are supportive of AN2 as a reasonable candidate *ent*-CPS with the potential to regulate induced kauralexin synthesis.

Spatial Regulation of Kauralexin Accumulation. To examine kauralexin distribution 24 h after *R. microsporus* elicitation, we consecutively removed 0.5-mm-thick layers from the treated site. Kauralexin accumulation was nearly exclusive to the top surface of the infected tissue (Fig. 3*F*). Phytoalexins often display highly localized accumulation at the site of infection to sterilize the area

against further pathogen entry (1). To examine kauralexin distribution in healthy untreated seedlings, we analyzed the roots, shoots, and scutella over a 2-wk developmental period. Early in the ontogeny of maize, the scutellum (or cotyledon) acts to absorb, store, and transfer nutrients from a collapsing endosperm to the developing seedling while preventing intrusion of soil microbes before senescence (35). A significant progressive accumulation of kauralexins, exceeding 150 μg·g⁻¹ FW, was specifically localized to the scutella (Fig. 3G). This suggests that kauralexins are also developmentally regulated; however, soil microorganisms may likewise elicit defense in the scutella. To examine if kauralexin biosynthesis is common in maize, we examined the genetic model B73 and 18 other diverse landrace inbred lines (36). At 10 d, we consistently detected high kauralexin levels, ranging from 50–167 μg·g⁻¹ FW, in the scutella of all lines examined (Fig. S5). Thus, kauralexins are widespread yet previously unknown metabolites in maize.

Kauralexins Display Antifungal and Insect Antifeedant Activity. To examine biological activity, we analyzed the growth curves of *R. microsporus* and *C. graminicola* in the presence of either
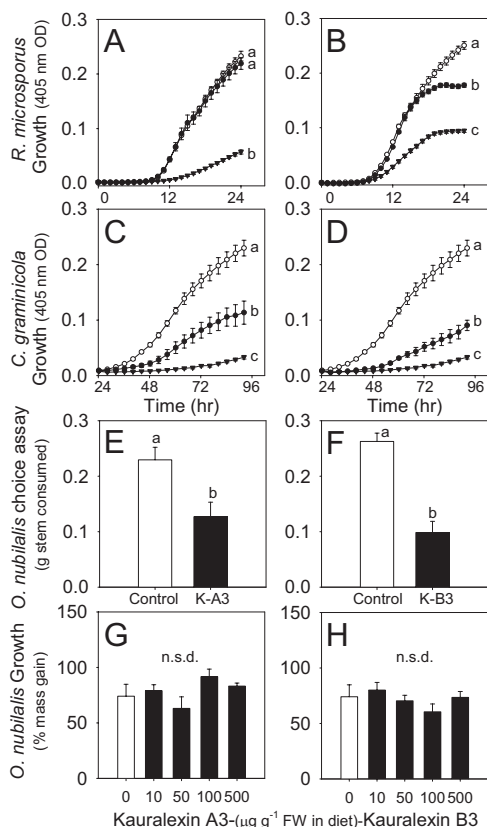
kauralexin A3 or B3 spanning a range of endogenous levels. After 24 h, 100 μg·mL⁻¹ kauralexin A3 resulted in a 75% average reduction in *R. microsporus* growth; however, 10 μg·mL⁻¹ was not active (Fig. 4A). Demonstrating activity at lower concentrations, both the 100- and 10-μg·mL⁻¹ doses of kauralexin B3 significantly reduced the growth of *R. microsporus* by 62% and 30%, respectively (Fig. 4B). Interestingly, although *C. graminicola* only weakly induces kauralexin accumulation (Fig. 2 *G–L* and Fig. S2B), its growth is greatly inhibited by accumulation of kauralexins (Fig. 4 *C* and *D*). On average, both kauralexin A3 and B3 inhibited the growth of *C. graminicola* by 50–60% and 85–90% at 10 and 100 μg·mL⁻¹, respectively. As in other *Colletotrichum* species, effectors secreted during the biotrophic phase of *C. graminicola* may be important in the suppression of these maize defense responses (37).

To address their potential defensive role against insects, we also examined the activity of kauralexins A3 and B3 on the feeding preference and growth of *O. nubilalis* using choice and nonchoice assays. Stem surfaces treated with 50 μg·g⁻¹ FW of kauralexins A3 and B3 significantly reduced the tissue consumed by *O. nubilalis* compared with the paired untreated control stem sections (Fig. 4 *E* and *F*). In this context, kauralexins act as local antifeedants. Using nonchoice artificial diet assays, kauralexins A3 and B3 were tested over a range of 10–500 μg·g⁻¹ FW but did not significantly inhibit insect growth as estimated by percentage of mass gain (Fig. 4 *G* and *H*). Similar results demonstrating Lepidoptera antifeedant activity without growth suppression have been reported for plant terpenoid defenses (38). In a natural situation, it is likely that kauralexins are associated with additional antinutritive substances (7).

Numerous lines of evidence have pointed to the existence of diterpenoid phytoalexins in maize. Over 30 y ago, Mellon and West (15) demonstrated that the *ent*-kaur-15-ene is synthesized by maize tissues exposed to fungal pathogens and foreshadowed the existence of related diterpenoid phytoalexins by stating that "The relatively polar fraction obtained from silicic acid chromatography of the lipids extracted from infected maize plants does contain antifungal substances... however, the nature of the active substance(s) in this impure fraction is not known." A quarter of a century later, Harris et al. (17) cloned and functionally characterized *An2*, an *F. graminearum*-inducible *ent*-CPS in maize. The demonstrated precedence of rice to produce diterpenoid phytoalexins also fueled the suspicion that *ent*-kaur-15-ene "may similarly serve as precursors to more elaborated, bioactive maize phytoalexins" (5). Kauralexins are ubiquitous in maize seedling scutella and can be induced over 2,000-fold following fungal infection (Fig. 3G and Fig. S2B). This pattern is curious, because rice diterpenoid phytoalexins were found constitutively in seed husks before the discovery of pathogen inducibility in leaves (5). Although we have addressed initial topics relating to biotic stimuli, structures, phytohormone regulation, localization, potential pathways, and biological activity, many questions remain. For example, are kauralexins the dominant metabolites accumulated or are there additional polar modifications not captured by these analyses? What are the activities of kauralexins against a wide range of biotic threats in different plant tissues throughout development? Do differences in maize kauralexin production provide mechanistic explanations for resistance in select maize lines? Development of homozygous lines harboring a null mutation in *An2* would greatly facilitate the critical examination of biosynthetic origin and, ultimately, function of these phytoalexins in multiple ecological contexts. Collectively, these results will likely provide a springboard into numerous functions of terpenoid phytoalexins in maize, which will likely match the established biological significance and complexities displayed in rice.

Fig. 4. Kauralexins display antifungal and insect antifeedant activities at physiologically relevant concentrations. Average (*n* = 8, ±SEM) *R. microsporus* growth time course in nutrient broth containing kauralexin A3 (*A*) and kauralexin B3 (*B*) at concentrations of 0 (○), 10 (●), and 100 (▼) μg·mL⁻¹ and, similarly, *C. graminicola* in the presence of kauralexin A3 (*C*) and kauralexin B3 (*D*). Average (*n* = 8, ±SEM) mass (grams) of maize stem consumed by *O. nubilalis* larvae in a 24-h choice assay containing 0 (Control) or 50 μg·g⁻¹ FW of kauralexin A3 (*E*) or, similarly, kauralexin B3 (*F*). K-A3, kauralexin A3; K-B3, kauralexin B3. Average (*n* = 6, ±SEM) 24-h growth (% mass gain) of *O. nubilalis* larvae on a diet containing a range of kauralexin A3 (*G*) or kauralexin B3 (*H*) concentrations. Within plots (*A–F*), different letters (a–c) represent significant differences (*P* < 0.01 for all ANOVAs; *P* < 0.05 for Tukey test corrections for multiple comparisons). Not statistically different (n.s.d.) indicates ANOVA *P* values >0.05.

Materials and Methods

Plant, Insect, and Fungal Materials. Hybrid maize (*Zea mays* var. Golden Queen; Southern States Cooperative, Inc.), landrace isogenic inbreds (CML322, CML69, Ms71, Ki11, Hp301, CML247, CML228, CML52, B73, Mo18W, B97, Ki3, CML103, NC350, NC358, CML277, Oh43, Tx303, and CML333; source information available at http://www.panzea.org/lit/germplasm.html), and *A. squamosa* (TARS-17880; US Department of Agriculture, Agricultural Research Service Tropical Agriculture Research Station) seeds were germinated in MetroMix 200 (Sun Gro Horticulture Distribution, Inc.) supplemented with 14-14-14 Osmocote (Scotts Miracle-Gro) and grown as previously described (18). *O. nubilalis* (Benzon Research, Inc.) were raised on an artificial diet at 29 °C and received as late first instars. Fungal stock cultures of *R. microsporus* (NRRL 54029), *C. graminicola* (strain M1.001), and *F. graminearum* (NRRL 31084) were grown on V8 agar for 2–3 wk before the quantification and use of spores (39).

Diterpenoid Isolation. Maize tissue (1.4 kg) infected by *R. microsporus* was ground to a powder, extracted with 3 L of 2:1 MeCl$_2$/propanol for 48 h, separated into organic and aqueous layers, and dried under vacuum. Material from the organic layer was flash-chromatographed on 30 g of bulk C18, washed with H$_2$O and 1:1 MeOH/H$_2$O, eluted with 100% MeOH, and dried under vacuum. The residue was then separated by preparative flash chromatography (CombiFlashR$_f$; Teledyne ISCO, Inc.) on a 150-g C18 (RediSepRF Gold) column using a H$_2$O/MeOH gradient and a flow rate of 60 mL·min^{-1}. Fractions highly enriched in kauralexins B2, B3, and A3 were eluted at 70%, 75%, and 80% MeOH, respectively, and dried under vacuum. Fractions were then solubilized in ethyl acetate (EtOAc), loaded onto 1 g of LC-Si SPE (Supelclean) columns, eluted with 1:1 EtOAc/hexane, and again dried under vacuum. Samples enriched in kauralexins A3 and B3 were then finally purified by HPLC using a Diol (250 mm × 4.6 mm, 5 µm; J. T. Baker Research Products) column with a flow rate of 1 mL·min^{-1} and a linear gradient of 100% pentane to 100% EtOAc over 30 min, yielding between 5 and 10 mg of pure white solid material after multiple injections. The enriched kauralexin B2 fraction was brought up in 220 µL of 5:5:1 EtOAc/MeCl$_2$/MeOH, derivatized with 10 µL of 2 M (trimethylsilyl)diazomethane, and dried under vacuum. The sample was then separated by HPLC using a Zorbax RX-silica (250 mm × 4.6 mm, 5 µm; Agilent) column with a flow rate of 1 mL·min^{-1} and a linear gradient of 100% pentane to 100% EtOAc over 30 min, resulting in purification of the kauralexin B2 C-17 monomethyl ester used for NMR analysis. At each step, the content and purity of fractions were analyzed as methyl esters by GC/MS.

Quantification of Maize Metabolites. Sample preparation via solvent extraction, methylation, vapor-phase extraction, and isobutane CI GC/MS-based stem tissue quantification of oxylipins was performed using previously developed methods (19). To include kauralexins in these analyses, we used a DB-35MS (30 m × 0.25 mm × 0.25 µm; Agilent) GC column held at 70 °C for 1 min after injection and then temperature-programmed at 15 °C min^{-1} to 300 °C (7 min), with helium as the carrier gas (0.7 mL·min^{-1}). The identity of OPEA was confirmed based on GC retention time and EI spectra comparison with an authentic standard (Larodan Fine Chemical AB). Kauralexin information is given in Fig. 1. Quantity estimates of OPDA, OPEA, and kauralexins were based on ^{13}C$_{18}$-linolenic acid.

Maize Stem Phytoalexin Elicitation Assays. Fungal and chemical elicitation assays used 21- to 28-d-old *Z. mays* var. Golden Queen grown in 1-L plastic

pots. Plants in damage-related treatment groups were slit in the center, spanning both sides of the stem, with a surgical scalpel that was pulled 8–10 cm upward to create a parallel longitudinal incision. This treatment spanned the upper nodes, internodes, and unexpanded leaves. All fungal spore inoculations (1 × 10^7 spores·mL^{-1}) and pectinase (0.1 g·mL^{-1}, from *Rhizopus* spp., CAS 9032-75-1; Sigma) treatments were performed in 100 µL of H$_2$O. Oxylipins (JA, OPDA, and OPEA) were applied at 100 nmol·plant^{-1} in 10 µL of H$_2$O as NH4$^+$ or Na$^+$ salts, and E-related treatments (EP, ethylphosphonic acid, phosphonic acid, and ACC) were applied at 33 nmol·plant^{-1} in 10 µL of H$_2$O. For the *O. nubilalis* stem herbivory trials, we used 32-d-old plants grown in 3 gallon (G) pots, each with 11–13 visible leaves. Plants were damaged by inserting a no. 1 cork borer 75% through the stem above the first basal node. Early sixth-instar larvae, previously maintained for 24 h on maize leaves, readily initiated feeding tunnels at this selected location. Each sample collected (*n* = 3) was a separate pool of three identically treated plants. Including a time 0 control, control, damage, and *O. nubilalis* samples were taken at 3, 12, 24, and 48 h.

RNA Isolation and *An2* qRT-PCR. Total RNA was isolated with TRIzol (Invitrogen) according to the manufacturer's protocol. First-strand cDNA was synthesized with the RETROscript reverse transcriptase kit (Ambion) using random decamer primers. qRT-PCR was performed using Power SYBR Green Master mix (Applied Biosystems), and 300 nM primers. Transcript levels of *An2* were quantified with the ABI 7300 sequence detection system (Applied Biosystems). Mean cycle threshold (Ct) values of triplicate reactions were normalized to *EF-1α* (GenBank accession no. AF136829) (40). Fold-change calculations were performed using the equation 2$^{-\Delta\Delta Ct}$ (41). qRT-PCR primers were as follows: *An2* Forward, 5′-TGTTCTTGTGAAGGCAGTTC-3′; *An2* Reverse, 5′-TCATTCGAGCTAAAAGCAGA-3′; *EF-1α* Forward, 5′-GCTTCACG-TCCCAGGTCATC-3′; and *EF-1α* Reverse, 5′-TAGGCTTGGTGGGTATCATC-3′.

Kauralexin Activity Assays. Antifungal assays were performed using the Clinical and Laboratory Standards Institute M38-A2 guidelines (42). In brief, a 96-well microtiter plate-based method using a Synergy4 (BioTech Instruments, Inc.) reader was used to monitor fungal growth at 37 °C in broth media through periodic measurements of changes in OD at 405 nm. Each well contained 200 µL of initial fungal inoculum (2 × 10^4 conidia·mL^{-1}) and 0.5 µL of EtOH. The insect choice assays used 3.5-cm-long stem sections from 30-d-old maize grown in 3-G pots. A longitudinal no. 1 cork borer hole was created down the center, followed by lengthwise sectioning into two weighed halves (~3 g each) and treatment with 3 µL of EtOH containing either 0 (control) or 50 µg·µL^{-1} purified kauralexins. Stem halves were rejoined with Parafilm M (Pechiney Plastic Packaging Company) and infested with one early sixth-instar *O. nubilalis*, and stem mass lost was determined 24 h later. For the nonchoice assays, early fourth-instar *O. nubilalis* larvae were allowed to feed on a commercial insect diet mixed with 0–500 µg·g^{-1} FW of kauralexin A3 or B3 for 24 h. All larvae were weighed immediately before and after the experiment to determine percentage of mass gain.

1. Smith CJ (1996) Accumulation of phytoalexins: Defence mechanism and stimulus response system. *New Phytol* 132:1–45.
2. Delannoy E, et al. (2005) Resistance of cotton towards *Xanthomonas campestris* pv. *malvacearum*. *Annu Rev Phytopathol* 43:63–82.
3. McAuslane HJ, Alborn HT (1998) Systemic induction of allelochemicals in glanded and glandless isogenic cotton by *Spodoptera exigua* feeding. *J Chem Ecol* 24:399–416.
4. Toyomasu T (2008) Recent advances regarding diterpene cyclase genes in higher plants and fungi. *Biosci Biotechnol Biochem* 72:1168–1175.
5. Peters RJ (2006) Uncovering the complex metabolic network underlying diterpenoid phytoalexin biosynthesis in rice and other cereal crop plants. *Phytochemistry* 67:2307–2317.
6. FAOSTAT (2010) Food and Agriculture Organization of the United Nations [online]. Available at http://faostat.fao.org/site/567/default.aspx. Accessed September 28, 2010.
7. McMullen MD, Frey M, Degenhardt J (2009) *Handbook of Maize: Its Biology*, eds Bennetzen JL, Hake SC (Springer, New York), pp 271–289.
8. Degenhardt J, et al. (2009) Restoring a maize root signal that attracts insect-killing nematodes to control a major pest. *Proc Natl Acad Sci USA* 106:13213–13218.
9. Turlings TCJ, Tumlinson JH, Lewis WJ (1990) Exploitation of herbivore-induced plant odors by host-seeking parasitic wasps. *Science* 250:1251–1253.
10. Gatch EW, Munkvold GP (2002) Fungal species composition in maize stalks in relation to European corn borer injury and transgenic insect protection. *Plant Dis* 86:1156–1162.
11. Keller NP, Bergstrom GC, Carruthers RI (1986) Potential yield reductions in maize associated with an Anthracnose European Corn-Borer pest complex in New York. *Phytopathology* 76:586–589.
12. Broglie KE, et al. (2009) Polynucleotides and methods for making plants resistant to fungal pathogens. US Patent 7619133.
13. Ostlie KR, Hutchinson WD, Hellmich RL (1997) *Bt Corn and European Corn Borer* (NCR-602, Extension Publication, University of Minnesota, St. Paul, MN), pp 1–18.
14. Kono Y, et al. (1991) Structures of Oryzalide-A and Oryzalide-B, and Oryzalic Acid-A, a group of novel antimicrobial diterpenes, isolated from healthy leaves of a bacterial leaf blight-resistant cultivar of rice plant. *Agric Biol Chem* 55:803–811.
15. Mellon JE, West CA (1979) Diterpene biosynthesis in maize seedlings in response to fungal infection. *Plant Physiol* 64:406–410.
16. Bensen RJ, et al. (1995) Cloning and characterization of the maize *An1* gene. *Plant Cell* 7:75–84.
17. Harris LJ, et al. (2005) The maize *An2* gene is induced by *Fusarium* attack and encodes an *ent*-copalyl diphosphate synthase. *Plant Mol Biol* 59:881–894.

PLANT BIOLOGY

18. Schmelz EA, Engelberth J, Alborn HT, Tumlinson JH, 3rd, Teal PEA (2009) Phytohormone-based activity mapping of insect herbivore-produced elicitors. *Proc Natl Acad Sci USA* 106:653–657.
19. Schmelz EA, et al. (2003) Simultaneous analysis of phytohormones, phytotoxins, and volatile organic compounds in plants. *Proc Natl Acad Sci USA* 100:10552–10557.
20. Yang YL, Chang FR, Wu CC, Wang WY, Wu YC (2002) New *ent*-kaurane diterpenoids with anti-platelet aggregation activity from *Annona squamosa. J Nat Prod* 65:1462–1467.
21. Bohlmann F, Kramp W, Jakupovic J, Robinson H, King RM (1982) Naturally-occurring terpene derivatives. Part 381. Diterpenes from *Baccharis* species. *Phytochemistry* 21: 399–403.
22. Ellmauerer E, Jakupovic J, Bohlmann F, Scott R (1987) Kaurane, isokaurane, and beyerane derivatives from *Peteravenia* species. *J Nat Prod* 50:221–224.
23. Henrick CA, Jefferies PR (1964) The chemistry of the Euphorbiaceae. VII. The diterpenes of *Ricinocarpos stylosus. Aust J Chem* 17:915–933.
24. Herz W, Kulanthaivel P, Watanabe K (1983) *Ent*-Kauranes and other constituents of 3 *Helianthus* species. *Phytochemistry* 22:2021–2025.
25. Liu KS (1994) Preparation of fatty-acid methyl esters for gas-chromatographic analysis of lipids in biological materials. *J Am Oil Chem Soc* 71:1179–1187.
26. Glazebrook J (2005) Contrasting mechanisms of defense against biotrophic and necrotrophic pathogens. *Annu Rev Phytopathol* 43:205–227.
27. Howe GA, Jander G (2008) Plant immunity to insect herbivores. *Annu Rev Plant Biol* 59:41–66.
28. Grechkin AN, et al. (2008) Tomato CYP74C3 is a multifunctional enzyme not only synthesizing allene oxide but also catalyzing its hydrolysis and cyclization. *ChemBioChem* 9:2498–2505.
29. Taki N, et al. (2005) 12-oxo-phytodienoic acid triggers expression of a distinct set of genes and plays a role in wound-induced gene expression in Arabidopsis. *Plant Physiol* 139:1268–1283.
30. De Wilde RC (1971) Practical applications of (2-chloroethyl) phosphonic acid in agricultural production. *HortScience* 6:364–370.
31. Zulak KG, et al. (2009) Targeted proteomics using selected reaction monitoring reveals the induction of specific terpene synthases in a multi-level study of methyl jasmonate-treated Norway spruce (*Picea abies). Plant J* 60:1015–1030.
32. Hudgins JW, Franceschi VR (2004) Methyl jasmonate-induced ethylene production is responsible for conifer phloem defense responses and reprogramming of stem cambial zone for traumatic resin duct formation. *Plant Physiol* 135:2134–2149.
33. Prisic S, Xu MM, Wilderman PR, Peters RJ (2004) Rice contains two disparate *ent*-copalyl diphosphate synthases with distinct metabolic functions. *Plant Physiol* 136: 4228–4236.
34. Doehlemann G, et al. (2008) Reprogramming a maize plant: Transcriptional and metabolic changes induced by the fungal biotroph *Ustilago maydis. Plant J* 56: 181–195.
35. Kiesselbach TA (1949) The structure and reproduction of corn. University of Nebraska, Agricultural Experimental Station Bulletin No. 161, 96 pp.
36. Yu JM, Holland JB, McMullen MD, Buckler ES (2008) Genetic design and statistical power of nested association mapping in maize. *Genetics* 178:539–551.
37. Stephenson SA, Hatfield J, Rusu AG, Maclean DJ, Manners JM (2000) CgDN3: An essential pathogenicity gene of *Colletotrichum gloeosporioides* necessary to avert a hypersensitive-like response in the host *Stylosanthes guianensis. Mol Plant Microbe Interact* 13:929–941.
38. Blaney WM, Simmonds MSJ, Ley SV, Anderson JC, Toogood PL (1990) Antifeedant effects of azadirachtin and structurally related compounds on Lepidopterous larvae. *Entomol Exp Appl* 55:149–160.
39. Leslie JF, Summerell BA (2006) *The Fusarium Laboratory Manual* (Blackwell Publishing, Ames, IA), 388 pp.
40. Kirchberger S, et al. (2007) Molecular and biochemical analysis of the plastidic ADP-glucose transporter (ZmBT1) from *Zea mays. J Biol Chem* 282:22481–22491.
41. Livak KJ, Schmittgen TD (2001) Analysis of relative gene expression data using real-time quantitative PCR and the 2(-Delta Delta C(T)) Method. *Methods* 25: 402–408.
42. Pfaller MA, et al. (2009) Wild-type MIC distribution and epidemiological cutoff values for *Aspergillus fumigatus* and three triazoles as determined by the Clinical and Laboratory Standards Institute broth microdilution methods. *J Clin Microbiol* 47: 3142–3146.